

COMPRESSIBLE FLOW SIMULATIONS FOR SHOCK TUBE PERFORMANCE ANALYSIS

Grace Lang

Professor Christopher Goyne, Advisor
University of Virginia

Abstract

Wind tunnels currently serve as testing facilities for spacecraft and high speed aircraft. The ability to simulate the flow of these experiments augments the results by providing additional data. This work focuses on simulations for a propulsion instrument shock tube laboratory (PISTL) at the University of Virginia Aerospace Research Laboratory. The project uses L1d3 numerical analysis software to create models representing facility dimensions and initial conditions for four flow fields. Post-processing of the resulting data into readable plots enables facility optimization by providing details about flow conditions. Space-time, pressure-position and pressure-time curves give insight into the behavior of the gasses in the shock tube and enable the identification of key instances during the experiment. From these points of interest, information on temperature, speed, density and pressure in the test section is determined.

Introduction

Traveling at hypersonic speeds, generally accepted as speeds greater than Mach 5, has many useful applications. Two main areas where hypersonics is important are 1) military/national defense and 2) planetary exploration/space access. At these speeds, intense aerodynamic heating presents new design challenges¹. Advancement in hypersonics is dependent on developing technology that can withstand high temperature conditions². Throughout the history of space flight, missions have been carried out that achieved these speeds. For example, the Apollo missions dealt with the implications of returning from the moon.

This led to the development of a new heat shield that could withstand reentry. Another crucial factor to this lunar achievement was the validation of the use of hypersonic testing facilities. It was found, through experimentation, that ground facilities could provide accurate estimations of flight results. This required the use of multiple wind tunnels that could produce a range of flow speeds within the hypersonic regime. Currently, interests lie with increasing safety and affordability of hypersonic flight. One way to achieve these goals is to use computational simulations in addition to ground experimentation¹. Computational simulations of ground test facilities also offer other benefits. These include the ability to: 1) test new facility parameters prior to altering the actual hardware, 2) gather additional information that could not be measured experimentally, and 3) verify new designs and experimental results³. Therefore, the use of detailed numerical analysis complements hypersonic testing. This research study uses a specific compressible flow simulation tool to gather more information on flow conditions of experiments to be run in a hypersonic ground test facility. There are three main research objectives utilizing the software: 1) to set-up the computing environment, 2) run simulations to predict the flow for established test conditions, and 3) create visualizations of the data to aid in the future use of the facility.

Background

Shock Tube Theory

One type of hypersonic ground test facility is a wind tunnel that operates as a shock tube. A shock tube works by creating a pressure difference between two sections separated with a diaphragm. The section that initially contains high pressure gas is known as the driver section, and the low pressure section is called the driven section, as seen in Figure 1 below.

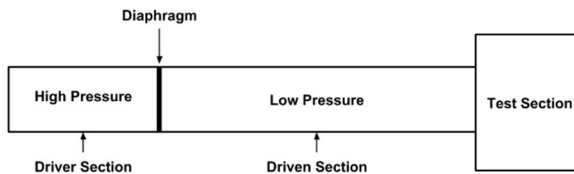


Figure 1: Pressure driven shock tube

Once the diaphragm bursts, an expansion wave propagates leftwards into the driver section, and a shock wave propagates rightwards into the driven section. The shock wave, travelling through the driven section, creates a flow of gas that can be used for hypersonic aerodynamics studies in the test section.

Before diaphragm rupture, the pressure-distance diagram for this scenario is a step function. However, as the shock wave travels rightward, the pressure of the gas increases as a step function. Conversely, the left-moving expansion wave continuously decreases the pressure to the value behind the wave. Therefore, as the waves travel outwards from the contact surface (interface between the two gases) the pressures begin to even out at a value between the two initial pressures. Once the shock wave moving rightward through the tube reaches the test section, it reflects and a new shock wave traveling left at a slower velocity is formed (in reflected shock tube mode). The velocity behind the reflected shock wave is zero. Wave diagrams (position-time) can be useful

to show this process and track a particle's change in position with respect to unsteady wave motion⁴.

Shock Tube Facility

The University of Virginia's Aerospace Research Laboratory has one of these facilities. Specifically, it has a 50 ft-long propulsion instrument shock tube laboratory (PISTL) that was originally developed by the NASA Langley Research Center. The facility can operate in shock tube and expansion tube mode. An image of the facility is shown in Figure 2.



Figure 2: PISTL facility at UVA

The wind tunnel has the capability to reach flow velocities above 4 km/s.⁵ This means that the facility is capable of simulation of atmospheric reentry and planetary entry conditions.

As discussed previously, the ability to apply computational methods to hypersonic research is necessary. The simulations of the facility located at the University of Virginia are achieved utilizing the L1d3 quasi-one-dimensional gas dynamics software developed at the University of Queensland. The results of a simulation follow directly from the initial conditions before diaphragm rupture, so the calculated flow field is

contingent upon an accurate representation of the facility setup.⁴ Utilizing a control mass cell, the numerical modeling is done by considering the rate of change of momentum and energy, and thermodynamic specifications of the properties of the gas³. Dividing the gas slugs into control mass cells in order to analyze properties is known as a Lagrangian discretization⁶. The program was validated by running simulations for simple systems where the outcome was known. It was found that the software could reliably capture shocks, the effect of area changes, and shock speed³. Therefore the installation, creation of simulations, and post-processing of flow data into readable configurations was the main focus of this research project and was carried out by using available documentation resources provide with the L1d3 software.

Methods

Set up of Computing Environment

In order to run the L1d3 software on a windows machine, a specific computing environment was needed. Ubuntu 17.10 was run in a virtual machine, and the source codes were cloned from a public Mercurial repository. Then 20 packages were installed to compile the code. To verify this computational setup, an example file provided by the creators of the software was run. The example contained an input script specifying the initial conditions for a gas accelerating a piston. After the simulation completed, the post processor created files that could be used to create space-time plots, position time plots, and extract data at specified history locations. The success of this example confirmed the correct setup of the computational environment.⁷

Simulations

To accomplish the second research objective, an input file was created that

specifies the initial conditions and dimensions of the shock tube. The software creators provided an example script for the Sod shock tube problem⁸. The structure of this example was used as a template for the input file created for the ARL facility. First, the gas model was chosen as a thermally perfect gas. The species Helium and Air were selected, and the ends of the tube were specified by x-location and diameter seen in Table 1.

Table 1: PISTL facility dimensions

<i>Location</i>	<i>Length (m)</i>	<i>Inner diameter (m)</i>
<i>Driver</i>	0.90	0.0889
<i>Diaphragm</i>	0.06	0.0889
<i>Driven</i>	3.80	0.0889

In the model, the diaphragm section does not have a thickness so 0.03m was added to the driver and driven sections to maintain the accurate tube length. Then the gas path was defined starting with the left wall of the tube, then the driver gas, interface, driven gas and right wall. Parameters set for each gas include pressure, mass fraction, velocity, and temperature. A total of four cases were run for different pressures of the driver and driven sections. They are specified in Table 2 by cases A-D.

Table 2: Established test conditions

<i>Case</i>	<i>Driver Pressure (MPa)</i>	<i>Driven Pressure (kPa)</i>
<i>A</i>	5.516	68.95
<i>B</i>	5.516	13.79
<i>C</i>	9.997	13.79
<i>D</i>	9.997	.3447

All of the parameters except for pressure were kept constant across all cases. This means the driver gas was always helium and the driven gas was air. The temperature was set to 70°F or approximately 294 K, and the initial velocities of both sections were zero.

The last section of the input script contains time-stepping parameters such as maximum simulation time, maximum steps, locations of interest on the tube, and the frequency of writing complete solutions.⁸ History locations were placed at the ends of the tube in order to see the flow conditions right before the primary shock reaches the test section and after the reflected shock. The length of the simulation was determined through trial and error utilizing a pressure vs. time plot for an x location at the end of the tube.

After the input script was completed, the simulation was run by a sequence of terminal commands. The first command created an input parameter file, followed by a file containing the initial flow solution at time=0 and a file containing the tube description. Lastly, the flow data was written in multiple files which could then be analyzed further.⁸

Post-Processing

The creation of data visualizations was accomplished through the use of programs within the L1d3 repository that extract flow data from the simulation file and output text files. Four programs were used in this process: `sptime.exe`, `l_post.exe`, `l_hist.exe`, and `mb_cont.exe`.⁸ The first three programs outputted text files, and the last program was used as a contour plotting tool. `Sptime.exe` was used to take the logarithm of the pressure at different positions and times throughout the experiment. The output of this program was used as the input to `mb_cont.exe`, which created the wave diagram for each simulation. `L_post.exe` was used to gather data on pressure vs. position at

five instances throughout the simulation. This spanned from $t = 0$ s to the time when the shock is reflected at the downstream end of the tube—which is different for each case. The last program, `l_hist.exe`, generated flow solutions for three points defined in the input file as a history location. The positions are: $x = 0.05$ m, $x = 4.60$ m, and $x = 4.75$ m. These points allowed for the creation of visualizations that showed when the waves (expansion, initial shock, and reflected shock) reached the ends of the tube by looking at pressure vs. time. Figure 3 shows these three history locations with respect to shock tube length.

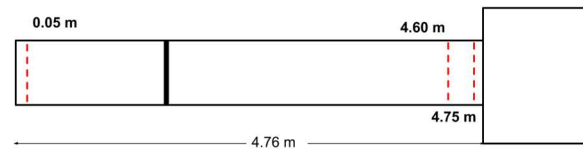


Figure 3: History locations for input file

The 0.05m history location captures flow conditions on the left end of the tube which is the behavior of the expansion wave. The 4.60 m and 4.75 m history locations capture the right end of the tube which is the behavior of the primary shock and reflected shock. These two locations represent the gas dynamics just before the shock reaches the test section. Therefore, the values at these points are indicators of the test conditions.

Results

A greater understanding of the flow conditions of the PISTL facility is possible through graphical representations of simulated experiments. These graphs are used to understand the behavior of the shocks, and to identify important instances during an experiment. Plotting techniques carried out for all four cases are discussed below for case A only. The same data processing method presented for case A was carried out for cases B and D. Results for case C are still in progress.

The space-time plot for case A can be seen in Figure 4.

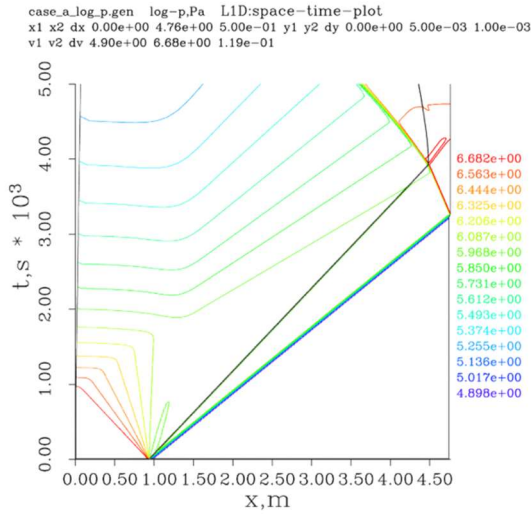


Figure 4: Space-Time plot case A

The simulation begins with the diaphragm rupture at $t = 0\text{s}$ and $x = 0.93\text{m}$. The expansion wave is represented in the bottom left corner of the plot. The decrease in pressure over time caused by the expansion is seen through the color change from red to green as the y-axis values increase. The bottom of the two lines with the positive slope shows the shock wave moving right from the rupture position. The inverse of the slope of this line corresponds to the speed of the wave. A rough estimate of the time the shock reaches in the end is 3.25 ms, which means the slope is approximately 0.00085—corresponding to a shock speed near 1177 m/s. The shock can then be seen reaching the end of the tube and is sent back in the other direction. The change in color of the line from blue to red, shows the increase in pressure that occurs as a result of the reflected wave.

A different perspective of the moving shock can be attained through a Pressure-Position plot. Figure 5 shows this relationship

for five 0.00085s intervals from 0.0s to 0.0034s.

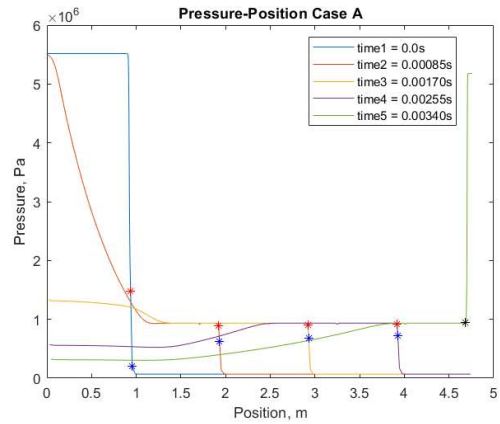


Figure 5: Pressure-Position plot case A

The final time of the plot coincides with the reflected shock, evident from the abrupt rise in pressure. This is consistent with the same increase in pressure seen in the space-time curve at the time of the reflected shock. Curves preceding the reflected shock represent the initial shock moving down the tube. The discrete step in the middle three curves at approximately 1 Pa is caused by the increase in pressure of the driven section once the shock passes. The expansion wave causes the more gradual change of pressure for each curve.

Red and blue markers were used to identify the exact position the shock passes for each time. Knowing the position and time allows for an accurate calculation of the shock speed. The two points were average for each curve and three velocities for the simulation were calculated and compared. The results are shown in Table 3.

Table 3: Shock Speeds for 3 intervals case A

Time interval	Speed (m/s)
Time1 to Time2	1168
Time2 to Time3	1172
Time3 to Time4	1172

The slight difference between the three speeds is insignificant, so the value from Time 3 to Time 4 was chosen as the shock speed for all cases. There is only a 0.5% difference between this speed and the estimate determined from the slope of the space-time curve. Table 4 shows the shock speeds determined for cases A, B and D.

Table 4: Shock speed case A-D

Case	Shock speed (m/s)
A	1172
B	1584
D	2734

The last visualization generated from the data is Pressure-Time for the history locations chosen in Figure 2. This plot, shown in Figure 6, gives insight into the flow conditions inside the test section.

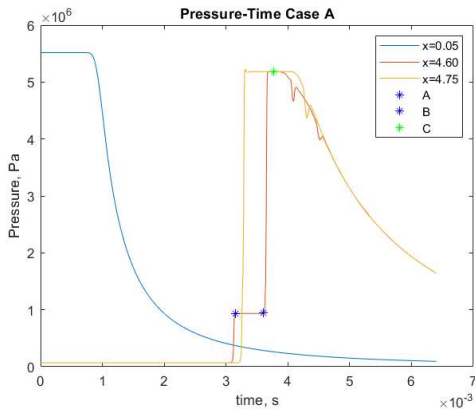


Figure 6: Pressure-Time plot case A

It also reinforces the previous discussion on the effect of the expansion wave on pressure: at $x = 0.05$ a continuous decrease in pressure over time is shown. Similarly, at the other end of the tube another continuous decrease in pressure occurs. This is caused by a reflected expansion wave reaching the right end of the tube. In addition, two instantaneous jumps in pressure are seen; first from the primary

shock and then from the reflected shock. Points A, B, and C were used to identify the time in which the waves pass the history locations and to determine thermodynamic properties. Specifically, gas speed, pressure, temperature and density were found at these two times at $x = 4.60$ m and averaged. It is assumed that these values represent the test conditions which would result in the test section if the tube were not operated in reflected shock tube mode. Table 5 shows the properties determined for cases A, B and D.

Table 5: Flow conditions after primary shock cases A, B and D

Case	Gas speed (m/s)	Gas pressure (kPa)	Gas Temp (K)	Gas density (kg/m ³)	Shock speed (m/s)
A	903.6	937	912	3.58	1172
B	1286	347	1393	0.87	1584
D	2217	23.6	3300	0.03	2734

The same properties were identified for the reflected conditions at point C and are shown in Table 6.

Table 6: Flow conditions after reflected shock cases A, B and D

Case	Gas speed (m/s)	Gas pressure (kPa)	Gas Temp (K)	Gas density (kg/m ³)
A	0.204	5184	1574	11.48
B	-1.616	2320	2559	3.159
D	1634	200.2	5695	0.126

It is necessary to note that the value for gas speed of Case D in Table 6 is 1634m/s, however the velocity after the reflected shock passes should be 0 m/s.⁴ The discrepancy between this value and the expected result may be due to the incorrect identification of the reflected shock on the Pressure-Time plot for Case D.

The test time of an experiment is also determined from this plot for reflected shock tube mode. Points A and B indicate the time the conditions are constant before the reflected shock passes the 4.60 m history location. The test time for cases A, B and D is shown in Table 7.

Table 7: Test time for cases A-D

Case	Test time (ms)
A	0.445
B	0.366
D	0.244

For post-processing, the gas was assumed to be calorically perfect. Stagnation temperature, gas speed of sound and gas Mach number are all calculated from values determined above.

The conservation of energy equation is used to find the stagnation temperature.

$$h_1 + \frac{u_1^2}{2} = h_2 + \frac{u_2^2}{2} \quad (1)$$

In equation 1, h represents enthalpy and u is velocity. Stagnation temperature occurs when the gas is brought to rest ($u=0$), and for a calorically perfect gas $h = C_p T$. Substituting in for these values, Equation 1 can be rewritten as:

$$C_p T_1 + \frac{u_1^2}{2} = C_p T_0 \quad (2)$$

Where T_1 is any point in the general flow field, and T_0 is the stagnation temperature. The speed of sound (a) is a function of temperature and is calculated using Equation 3.

$$a = \sqrt{\gamma RT} \quad (3)$$

Mach number is a function of the speed of sound and the gas speed and is calculated for the gas using Equation 4.⁴

$$M = \frac{u}{a} \quad (4)$$

The results from performing these calculations are presented in Table 8 for cases A, B and D.

Table 8: Calculated flow conditions cases A-D

Case	Stagnation Temp (K)	Gas Mach number	Gas speed of sound (m/s)
A	1320	1.495	604.9
B	2220	1.723	746.7
D	5756	1.928	1149

Conclusion and Further Research

In this work, flow is predicted for established test conditions through the implementation of the L1d3 software at the University of Virginia Aerospace Research Laboratory. Multiple models are created to simulate a diaphragm bursting in the PISTL facility for various initial pressures of driver and driven gases. This leads to the development of plots relating pressure, time, and position to be used as tools for understanding the operating conditions of an experiment. These graphs enable facility optimization by providing sufficient information for data analysis and calculations of additional flow properties.

Verification of the flow conditions must still be performed. The PISTL facility will be run for each of the established test conditions. A comparison of the experimental results with the simulation predictions will provide insight into the accuracy of the models. If proven correct, additional models can be created to simulate new experiments, and the full operational envelope of the facility can be explored.

The advancement of hypersonic vehicles through the application of numerical analysis software may result in the technology being affordable, reliable, and useful in the future. Applying this technique to the facility at UVA has the potential to shape future designs of high speed flight vehicles, both within and outside the atmosphere.

Acknowledgements

This research was funded by the Virginia Space Grant Consortium. The author would like to thank Professor Christopher Goyne of the University of Virginia for his assistance throughout the process. The L1D code was provided by the University of Queensland and Dr. Peter Jacobs provided valuable advice.

References

- [1] Heppenheimer, T. A. (2007). *Facing the Heat Barrier a history of hypersonics*. Washington, DC: National Aeronautics and Space Administration.
- [2] Lu, F. K., & Marren, D. E. (2002). *Advanced hypersonic test facilities*. Reston, VA: American Institute of Aeronautics and Astronautics.
- [3] Jacobs PA. (1994) *Quasi-one-dimensional modelling of a free-piston shock tunnel*. AIAA Journal, 1994; 32(1):137-145
- [4] Anderson, J. D., Jr. (1990). *Modern Compressible Flow with historical perspective* (2nd ed.). McGraw-Hill.
- [5] Goyne C. (2013) *Proposed New Hypersonic Aerodynamics and kHz Velocimetry Instrumentation Capabilities at UVa*. The University of Virginia
- [6] Jacobs PA. (1998) *Shock tube modelling with L1d*. The University of Queensland, Department of Mechanical Engineering Report 13/98, 1998
- [7] Getting the codes and preparing to run them — Compressible Flow CFD 3

documentation. (n.d.). Retrieved March 29, 2019, from <http://cfcfd.mechmining.uq.edu.au/getting-started.html>

[8] Jacobs PA. (2005) *Using l_script to define L1d simulations*. The University of Queensland, Centre for Hypersonics, Mechanical Engineering Report 2005/09